Available online at www.sciencedirect.com
SCIENCE DIRECT
Bioorganic & Medicinal Chemistry Letters
Bioorganic & Medicinal Chemistry Letters 16 (2006) 1353–1357

Triazolo[1,5-*a*]pyrimidines as novel CDK2 inhibitors: Protein structure-guided design and SAR

Christine M. Richardson,* Douglas S. Williamson, Martin J. Parratt, Jenifer Borgognoni, Andrew D. Cansfield, Pawel Dokurno, Geraint L. Francis, Rob Howes, Jonathan D. Moore, James B. Murray, Alan Robertson, Allan E. Surgenor and Christopher J. Torrance

Vernalis (R&D) Ltd., Granta Park, Great Abington, Cambridge CB1 6GB, UK

Received 10 October 2005; revised 11 November 2005; accepted 14 November 2005
Available online 1 December 2005
Communicated by Stephen Neidle

Abstract—Crystallographic and modelling data, in conjunction with a medicinal chemistry template-hopping approach, led to the identification of a series of novel and potent inhibitors of human cyclin-dependent kinase 2 (CDK2), with selectivity over glycogen synthase kinase-3β (GSK-3β). One example had a CDK2 IC_{50} of 120 nM and showed selectivity over GSK-3β of 167-fold.

Cyclin-dependent kinases (CDKs) are important for cell cycle control. When activated by phosphorylation and bound to the appropriate cyclin partner, they promote progress from G1 to S and from G2 to M (CDK inactivation is required for exit from mitosis). The central role of CDKs in driving cell cycle progression supports the hypothesis that CDK inhibitors will be useful in anticancer treatment. One compound, roscovitine **1**,[1] is in advanced clinical trials for this indication. None of the CDK inhibitors disclosed to date are entirely specific for a particular CDK. As the results from knock-out mice imply substantial functional redundancy in the CDK family, some degree of inhibitor promiscuity is probably desirable. Structure-guided drug design against CDK targets has largely focussed on CDK2, as its crystal structure has been available since 1993.[2] CDK2 is now thought to be dispensable for tumour formation and maintenance.[3,4] Fortunately, sequence alignment and homology modelling indicate a high degree of similarity between the active site of CDK2 and that of CDK1, the kinase most likely to replace missing CDK2 activity.[5] Only two of the 28 residues bounding the ligand binding site are not strictly conserved (H84S and Q85M) and neither of these side-chain switches would directly modify the active site, which implies that identification of compounds targeting CDK1 as well as CDK2 is likely. Therefore, we considered that using a structure-guided strategy based on CDK2 was an appropriate means to generate CDK inhibitors that might prove useful for the therapy of proliferative disorders.

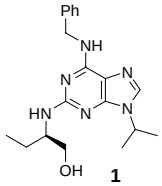

1

A medium-throughput screening campaign against a library of 3341 commercial compounds identified the pyrazolo[1,5-*a*]pyrimidine **2** (CDK2 IC_{50} 1.8 μM, HCT116 GI_{50} 8 μM).[6–9] Lead optimisation of the resulting series of pyrazolo[1,5-*a*]pyrimidine CDK2 inhibitors has been previously reported.[10] Given the intensely competitive nature of the CDK2 arena, however, there was a need to consider more novel scaffolds, and so a structure-guided medicinal chemistry strategy was employed to

Keywords: Structure-guided drug design; CDK2; Triazolo [1,5-*a*]-pyrimidines; SAR; Potency; Selectivity.
* Corresponding author. Tel.: +44 1223 895434; fax: +44 1223 895556; e-mail: c.richardson@vernalis.com

0960-894X/$ - see front matter © 2005 Elsevier Ltd. All rights reserved.
doi:10.1016/j.bmcl.2005.11.048

address this. One aspect of this strategy was to consider core templates which maintained similar interactions to the pyrazolo[1,5-*a*]pyrimidine but which were free from blocking IP; a so-called template-hopping strategy. The work reported here concerns SAR around one novel series of CDK2 inhibitors which resulted from this approach.

Early modelling work on the pyrazolo[1,5-*a*]pyrimidine **2**, using the proprietary code rDock (formerly called RiboDock),[11] subsequently verified by X-ray crystallography, suggested a binding mode where the bicyclic system was located in the ATP binding site, making polar interactions with the kinase binding motif. This comprises the backbone NH and carbonyl of Leu83 and the backbone carbonyl of Glu81, with the interaction between the Glu backbone and the ligand being a C–H···O hydrogen bond, which is now well recognized[12] as an important type of intermolecular interaction, particularly in the kinase field. Replacement of the ligand C3 atom with nitrogen results in a triazolo[1,5-*a*]pyrimidine scaffold, where the key interactions can be maintained, and which is amenable to substitution at the desired positions. Compound **3**, the triazolo[1,5-*a*]pyrimidine variant of **2**, was synthesised. This had a CDK2 IC_{50} of 26 μM, CDK1 IC_{50} 8.8 μM and HCT116 GI_{50} >80 μM, with conservation of binding mode verified by X-ray crystallography.

A large number of crystal structures are available on human CDK2 in complex with small ligands which bind deeply within the ATP site, and which interact with the kinase motif. An initial strategy involved exploration of the extent to which side chains present in other ligand series may be transferable to the new template. Of particular interest was NU6102 (**4**),[13] the CDK2 complex of which (pdb code: 1h1s) is available from the PDB.[14] A structural overlay of the bound pyrazolo[1,5-*a*]pyrimidine **2** with the structure of the NU6102 (**4**) complex suggested that the ligand templates did not directly coincide, but were offset in order to satisfy a common interaction pattern with the protein backbone. A direct side-chain replacement strategy might not, therefore, provide the optimal gain in potency.

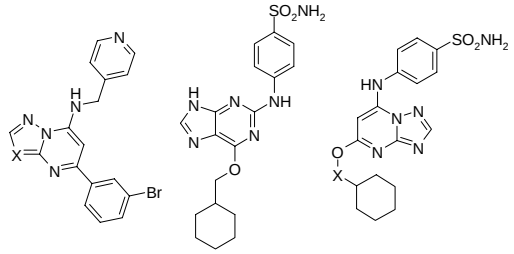

2 X = CH
3 X = N

4

5 X = CH_2
6 X = $[CH_2]_0$

Compound **5** was synthesised with the directly equivalent side chains, whilst compound **6** was made with a shorter side chain, as suggested by the structural overlays. The CDK2 assay data (Table 1) clearly show the shorter side chain to be preferred, consistent with the hypothesis, with an increase in potency of 32-fold. Compound **6** also showed good activity against CDK1, with an IC_{50} of 140 nM. The proposed binding modes, obtained using rDock,[11] were verified by X-ray crystallography. Figure 1 shows the overlay of compound **6** with NU6102 (**4**), as determined from overlays of the two protein–ligand complexes, and with interactions to the central templates highlighted. The crystal structure of compound **6** in human CDK2 shows that the aryl sulfonamide packs against the backbones of His84 and Glu85, with the sulfonamide oxygens interacting with the backbone NH of Asp86 (3.12 Å) and the side chain of Lys89 (3.2 Å) and the nitrogen of the sulfonamide being in proximity to the side chain of Asp86 (3.4 Å), although with a relatively poor geometry for a hydrogen bonding interaction. The cyclohexyl group of compound **6** packs against a relatively hydrophobic surface involving Ile10, Val18 and Gln131 and the backbones of Gly11 and Glu12, where the polar atoms are orientated orthogonal to the ligand. There is an additional interaction, not seen in the NU6102 (**4**) complex, from Lys33 (3.06 Å) to the triazolo[1,5-*a*]pyrimidine ring. It is interesting to note that, whilst the interactions to the core template are conserved and the aryl sulfonamide binds to a similar region of the active site, when comparing the complexes of compound **6** and NU6102 (**4**) with CDK2, the *O*-cyclohexyl units are slightly offset in the crystal structures. The comparison in Figure 1 shows NU6102 as obtained from the activated CDK2-cyclin A structure, whilst compound **6** is taken from the complex with monomeric CDK2. This overlay is depicted, as it best shows the similarity in chain length between the substituents in compound **6** and NU6102. Comparisons have also been undertaken between compound **6** in the active form of CDK2 and NU6102 (**4**) in the active (1h1s derived) form, and between the complexes of compound **6** and NU6102 (**4**) in the inactive form of CDK2 as obtained in-house. Whilst the binding modes for the core and the aryl sulfonamide moieties are conserved, the cyclohexyl group shows some differences in orientation between the different structures. This is consistent with results from docking work on compound **6**, which suggested that the linker between the triazolo[1-5*a*]pyrimidine core and the cyclohexyl group was flexible, and that the cyclohexyl moiety could make favourable interactions with a number of residues in the active site.

Although the crystal structures of compounds **5** and **6** were prepared by soaking into crystals of apo-CDK2,[2] some protein flexibility can be seen, with both ligands appearing to mould the dynamic, glycine-rich loop (residues Ile10 to Tyr19) which borders the active site, as illustrated in Figure 2.[16]

Optimisation of the triazolo[1,5-*a*]pyrimidine series was undertaken, with the aim of improving potency for CDK2 and selectivity over glycogen synthase kinase-3β (GSK-3β), the main counterscreen. This was selected, since CDK2 and GSK-3β have therapeutically antagonistic effects, but also exhibit some similarities[17] in their small molecule inhibition profiles. Optimisation was achieved using the synthetic approach outlined in Scheme 1. The 7-Cl of 5,7-dichloro[1,2,4]-triazolo[1,5-*a*]pyrimidine

Table 1. Enzyme activity (CDK2, GSK-3β and CDK1), cell-based inhibition in HCT116 (colon) cell line and calculated Slog*P* values for triazolo[1,5-*a*]pyrimidines **5**, **6** and **11**–**17**

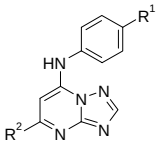

Compound	R^1	R^2	CDK2 IC_{50} (μM)[a,b]	GSK-3β IC_{50} (μM)[c]	CDK1 IC_{50} (μM)[b]	HCT116 GI_{50} (μM)	Slog*P*[d]
5	$-SO_2NH_2$	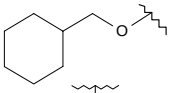	11	29	—	11	2.5
6	$-SO_2NH_2$	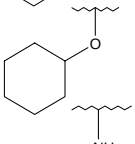	0.35	0.19	0.14	25	2.2
11	$-SO_2NH_2$	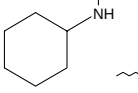	0.73	0.97	—	31	1.8
12	$-SO_2NH_2$	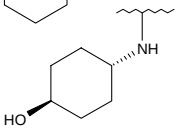	7.4	—	—	39	0.77
13	$-SO_2NH_2$	Et_2N	0.40	11	3.4	23	1.2
14	$-SO_2NH_2$	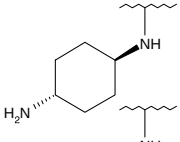	0.27	0.78	—	>80	0.74
15	$-SO_2NMe_2$	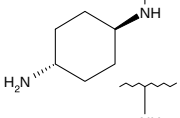	0.12	20	5.6	>80	1.3
16	$-SO_2Me$	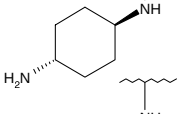	0.25	43	16	>80	1.5
17	$-SO_2Ph$	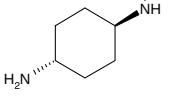	0.26	50	4.3	>80	2.9

[a] All IC_{50} and GI_{50} values are means of at least two determinations and are rounded to two significant figures where appropriate.
[b] [ATP] 100 μM (K_m 50 μM).
[c] [ATP] 10 μM (K_m 10 μM).
[d] Calculated with MOE.[24,25]

7[18] underwent facile displacement with a range of amines to afford compounds of type **8**. The 5-Cl then underwent Suzuki coupling with boronic acids in the presence of sodium carbonate and tetrakis(triphenylphosphine)palladium(0) in 1,4-dioxane and water in a Smith Synthesizer™ at 150 °C, to afford compounds of type **9** (R^2 = Ar). Alternatively, ethers of type **10** (X = O) could be synthesised by treating the chloride **8** in 1,4-dioxane and acetonitrile with an alcohol in the presence of sodium hydride and then heating the resulting mixture in a microwave reactor at 150 °C. The 5-Cl could also be displaced with amines by heating in a microwave reactor at 150 °C in ethanol, resulting in compounds of type **10** (X = NR^3).

Modification of the C5 side chain of compound **6** was investigated, as shown in Table 1. All the 5-position substituents comprising a heteroatom and a cyclohexyl ring were tolerated, with the exception of compound **12**, where the presence of a *trans*-4-OH group resulted in a 10-fold loss in CDK2 potency. This is in line with SAR published around NU6102 and its parent, NU2058.[19,20] The *N*,*N*-diethyl C5 substituent of compound **13** was also well tolerated. The *trans*-4-aminocyclohexylamino moiety, as found in H717 (**18**),[21] a potent and selective CDK2 inhibitor, was found to be particularly beneficial for CDK2 potency. The sensitivity of the primary sulfonamide to modification was also studied. N-Alkylation of the primary sulfonamide or

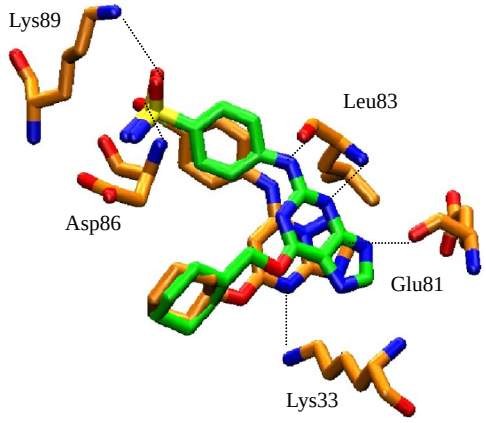

Figure 1. Overlay of NU-6102 (**4**) in green with compound **6** in orange. Residues involved in interactions to the templates (Lys89, Asp86, Lys33, Glu81 and Leu83) shown in stick representation.[15]

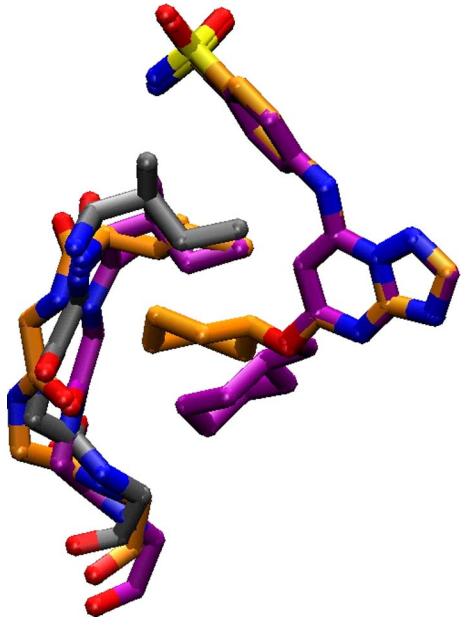

Figure 2. Overlaid complexes with compound **5** (carbon atoms in magenta), and compound **6** (carbons in orange) with the native structure with carbon atoms in grey. Backbone from Ile10 to Gly13 shown, with Ile10 side chain.[15]

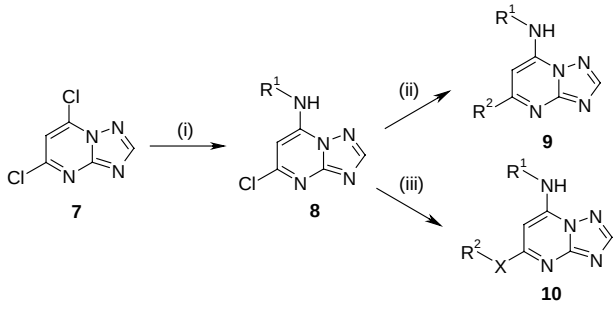

Scheme 1. Reagents and conditions: (i) R^1NH_2, MeOH, rt, 60–81%; (ii) $R^2B(OH)_2$, Na_2CO_3, $Pd(PPh_3)_4$, 1,4-dioxane, H_2O, microwave at 150 °C, 30 min, 12–35%; (iii) (for X = O) R^2OH, NaH, 1,4-dioxane, MeCN, microwave at 150 °C, 40 min, 9–12%; (for X = NR^3) R^2R^3NH, EtOH, microwave at 150 °C, 30 min, 4–64%.

removal of the nitrogen to form a sulfone was tolerated, with no significant loss in CDK2 potency, as can be seen by comparing compound **14** with **15**, **16** and **17**. This is consistent with the observation that the ligand sulfonamide moiety is interacting with the backbone of Asp86 and the interaction from the sulfonamide nitrogen to the side chain of this residue is poor. Compound **15** was the most potent and selective example, with a CDK2 IC_{50} of 120 nM and a GSK-3β IC_{50} of 20 μM, a selectivity of 167-fold. The GSK-3β selectivity is mediated, in part, by the Asp86 to Thr138 switch, which influences interaction to the ligand sulfonamide group. In addition, comparison of the CDK2 complex with a crystal structure of GSK-3β[22] shows that there is a different conformational preference in the loops bounding the cyclohexylamine binding site, which would necessitate a different ligand conformation in this region and disrupt the recognition of the side-chain amine.

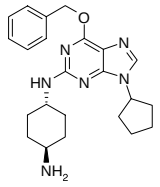

18

A subset of compounds showed selectivity against Chk1 and PDK1, unlike NU6102 (**4**), which hits Chk1 and PDK1 with IC_{50} <500 nM, and which is similarly potent against GSK-3β (IC_{50} 40 nM) and CDK2 (80 nM).[23] Compound **14** was highly selective, with a Chk1 IC_{50} of 93 μM and PDK1 IC_{50} of 43 μM, as was compound **15**, which had a Chk1 IC_{50} of 21 μM and PDK1 IC_{50} >200 μM. Compound **17** was less discriminatory, with selectivity over CDK2 of 8.5-fold for Chk1 and 54-fold for PDK1. Only compound **6** was more potent against CDK1, but all compounds do show some inhibition, although at a lower level than might be anticipated from a comparison of the protein structure alone. These results broadly support the hypothesis that a structure-guided strategy against CDK2 can give rise to inhibitors with a degree of activity against other members of the CDK family.

Unlike the corresponding pyrazolo[1,5-*a*]pyrimidines,[10] the triazolo[1,5-*a*]pyrimidines showed disappointing activity against human colon tumour cells, with only 5 of the 10 examples in Table 1 having an HCT116 GI_{50} <80 μM. The most potent of these was compound **5**, which had a GI_{50} of 11 μM against HCT116 cells. This value was extremely similar to its CDK2 IC_{50} (also 11 μM), however, which suggests that a different mode of action may be responsible for its cytotoxic effect. Efforts were made to improve the cellular potency of the series by increasing logP, but unfortunately this did not correlate with an improvement in HCT116 GI_{50}. For example, replacement of the methyl group of compound **16** with a phenyl ring afforded compound **17**, which had an SlogP[24,25] >1 unit higher and had enzyme potency similar to that of the methyl sulfone **16**, but both compounds were also equally inactive in cells.

In conclusion, a template-hopping approach guided by modelling and crystallographic data led to the rapid identification and initial optimisation of a novel series of CDK2 inhibitors. The relative activities of compounds **5** and **6** clearly demonstrate the role which protein structure-guided approaches can perform in aiding lead optimisation. Further optimisation afforded compound **15**, with a CDK2 IC_{50} of 120 nM and selectivity over GSK3β of 167-fold.

Acknowledgments

The authors thank Justin Bower for the re-synthesis of NU-6102 (**4**), Peter Kierstan, Kate Grant, Joanne Wayne and Angela Wheatley for running enzyme and cell-based assays, Steven Athwal and Mhairi Donohoe for production of CDK2, Adam Hold and Heather Simmonite for analytical support and James Davidson for his assistance in the preparation of this manuscript.

References and notes

1. Meijer, L.; Raymond, E. *Acc. Chem. Res.* **2003**, *36*, 417.
2. De Bondt, H. L.; Rosenblatt, J.; Jancarik, J.; Jones, H. D.; Morgan, D. O.; Kim, S.-H. *Nature* **1993**, *363*, 595.
3. Méndez, J. *Cell* **2003**, *114*, 398.
4. Pagano, M.; Jackson, P. K. *Cell* **2004**, *118*, 535.
5. Martin, A.; Odajima, J.; Hunt, S. L.; Dubus, P.; Ortega, S.; Malumbres, M.; Barbacid, M. *Cancer Cell* **2005**, *7*, 591.
6. All kinases from Upstate Ltd.; http://www.upstate.com.
7. Kinase assays were adapted from the following generic protocol, with ATP concentrations stated in the footnotes to Table 1; Lane, M. E.; Yu, B.; Rice, A.; Lipson, K. E.; Liang, C.; Sun, L.; Tang, C.; McMahon, G.; Pestell, R. G.; Wadler, S. *Cancer Res.* **2001**, *61*, 6170.
8. Skehan, P.; Storeng, R.; Scudiero, D.; Monks, A.; McMahon, J.; Vistica, D.; Warren, J. T.; Bokesch, H.; Kenney, S.; Boyd, M. R. *J. Natl. Cancer Inst.* **1990**, *82*, 1107.
9. GI_{50} is the inhibitor concentration which reduced tumour cell growth by 50% over 72 h. HCT116 is a colon carcinoma cell line, which is wild type with respect to p53 and Rb.
10. Williamson, D. S.; Parratt, M. J.; Bower, J. F.; Moore, J. D.; Richardson, C. M.; Dokurno, P.; Cansfield, A. D.; Francis, G. L.; Hebdon, R. J.; Howes, R.; Jackson, P. S.; Lockie, A. M.; Murray, J. B.; Nunns, C. L.; Powles, J.; Robertson, A.; Surgenor, A. E.; Torrance, C. J. *Bioorg. Med. Chem. Lett.* **2005**, *15*, 863.
11. Morley, S. D.; Afshar, M. *J. Comput. Aided Mol. Des.* **2004**, *18*, 189.
12. Pierce, A. C.; Sandretto, K. L.; Bemis, G. W. *Proteins* **2002**, *49*, 567.
13. Davies, T. G.; Bentley, J.; Arris, C. E.; Boyle, F. T.; Curtin, N. J.; Endicott, J. A.; Gibson, A. E.; Golding, B. T.; Griffin, R. J.; Hardcastle, I. R.; Jewsbury, P.; Johnson, L. N.; Mesguiche, V.; Newell, D. R.; Noble, M. E. M.; Tucker, J. A.; Wang, L.; Whitfield, H. J. *Nat. Struct. Biol.* **2002**, *9*, 745.
14. Berman, H. M.; Westbrook, J.; Feng, Z.; Gilliland, G.; Bhat, T. N.; Weissig, H.; Shindyalov, I. N.; Bourne, P. E. *Nucleic Acids Res.* **2000**, *28*, 235.
15. Humphrey, W.; Dalke, A.; Schulten, K. *J. Mol. Graph.* **1996**, *14*, 33, Available from http://www.ks.uiuc.edu/Research/vmd/.
16. PDB entry codes for deposited structures: Compound **2**, 2c68 (1.95 Å); compound **3**, 2c69 (2.1 Å); compound **4**, 2c6o (2.1 Å); compound **5**, 2c6i (1.8 Å); compound **6**, 2c6m (1.9 Å); compound **6** (cyclin A complex), 2c6t (2.6 Å); compound **11**, 2c6k (1.9 Å); compound **14**, 2c6l (2.3 Å).
17. Knight, Z. A.; Shokat, K. M. *Chem. Biol.* **2005**, *12*, 621.
18. Makisumi, Y.; Watanabe, H.; Tori, K. *Chem. Pharm. Bull.* **1964**, *12*, 204.
19. Gibson, A. E.; Arris, C. E.; Bentley, J.; Boyle, F. T.; Curtin, N. J.; Davies, T. G.; Endicott, J. A.; Golding, B. T.; Grant, S.; Griffin, R. J.; Jewsbury, P.; Johnson, L. N.; Mesguiche, V.; Newell, D. R.; Noble, M. E. M.; Tucker, J. A.; Whitfield, H. J. *J. Med. Chem.* **2002**, *45*, 3381.
20. Hardcastle, I. R.; Arris, C. E.; Bentley, J.; Boyle, T. F.; Chen, Y.; Curtin, N. J.; Endicott, J. A.; Gibson, A. E.; Golding, B. T.; Griffin, R. J.; Jewsbury, P.; Menyerol, J.; Mesguiche, V.; Newell, D. R.; Noble, M. E. M.; Pratt, D. J.; Wang, L.-Z.; Whitfield, H. J. *J. Med Chem.* **2004**, *47*, 3710.
21. Dreyer, M. K.; Borcherding, D. R.; Dumont, J. A.; Peet, N. P.; Tsay, J. T.; Wright, P. S.; Bitonti, A. J.; Shen, J.; Kim, S.-H. *J. Med. Chem.* **2001**, *44*, 524.
22. ter Haar, E.; Coll, J. T.; Austen, D. A.; Hsiao, H.-M.; Swenson, L.; Jain, J. *Nat. Struct. Biol.* **2001**, *8*, 593, PDB code 1I09.
23. In-house data.
24. MOE is available from the Chemical Computing Group; http://www.chemcomp.com/.
25. Wildman, S. A.; Crippen, G. M. *J. Chem. Inf. Comput. Sci.* **1999**, *39*, 868.